Available online at www.sciencedirect.com
SCIENCE DIRECT®
Mechanism and Machine Theory 41 (2006) 656–670
Mechanism and Machine Theory
www.elsevier.com/locate/mechmt

Screw theory tools for the synthesis of the geometry of a parallel robot for a given instantaneous task

Alon Wolf *, Moshe Shoham

Faculty of Mechanical Engineering, Technion—Israel Institute of Technology, Technion City, Haifa 32000, Israel

Received 16 September 2004; received in revised form 9 August 2005; accepted 14 September 2005
Available online 21 November 2005

Abstract

This investigation deals with the optimization of the kinematic parameters of a parallel robot structure, with respect to a given instantaneous twist deformation (ITD) of the moving platform. Drawing principally upon tools from screw theory, a parametric objective function is derived which quantifies the robots' performance with respect to the given ITD. Physically, the objective function quantifies the instantaneous work generated by the robotic structure via its platform, while the latter undergoes an instantaneous motion in the twist direction. The parameters which are optimized represent the pose of the robots platform and the geometry of the robot. This method can be used as one of other criterions in the design stage of a task-oriented new robot, while performing ITD using a fixed geometry robot or when using a reconfigurable robotic structure capable of changing its geometry to perform an ITD. The proposed algorithm is demonstrated on the Stewart platform and the 3-UPU parallel robot as examples.

Keywords: Parallel robot optimization; Screw theory; Reconfigurable robot

1. Introduction

Parallel robots are becoming a niche product in several robotics research areas, such as in machine tools, assembly lines, and medical applications. Numerous studies that investigate parallel mechanisms emphasize the various advantages of these mechanisms; however they also stress that these structures exhibit relatively more complex kinematics behavior when compared to serial robots. Hence, both the design and the operation of a parallel robot are more difficult than of a serial robot, from mechanical and control aspects. The performance of parallel robots near or at singular configuration is one example that highlights their complex behavior. In these configurations, the structure cannot balance an external wrench applied to the mobile platform, hence it tends to lose its stiffness while gaining extra degrees of freedom [1–3].

* Corresponding author. Tel.: +972 4 8293264; fax: +972 4 8324533.
E-mail address: alonw@tx.technion.ac.il (A. Wolf).

0094-114X/$ - see front matter
doi:10.1016/j.mechmachtheory.2005.09.006

This report extends the work done by Wolf and Shoham [4]. In their work, the authors applied line geometry and screw theory tools for the analysis of parallel robots. The authors also show that at any given robot configuration the sum of the reciprocal product of the rows of the Jacobian matrix, J which represents the instantaneous wrenches applied to the structure due to the ITD performed by the platform, indicates the total instantaneous work generated by the mechanical structure on the moving platform for the given ITD. Moreover, the paper also presents a method to identify the ITDs of the platform that minimize the instantaneous work. The current investigation elaborates on the tools presented in [4] and introduces new criteria for design of parallel robots. For this algorithm, we introduce an objective function that quantifies the total instantaneous work that the links of the robot apply to the moving platform while the latter moves instantaneously in a given ITD direction. This objective function is then minimized or maximized, according to the task requirements, to reveal optimal platform pose and geometrical dimensions of the robot.

Numerous investigations deal with the optimization of parallel robot structure. In [5] the authors introduce an optimization algorithm which maximizes the actual workspace that the mechanism covers relatively to the prescribed one. This is achieved by maximizing the intersection between these two workspaces. Other works in this area attempt to optimize the robot dexterity. In [6], the authors define the kinematic parameters of a parallel robot while in a given configuration, by maximizing the reciprocal of its condition number. A more general approach termed a global dexterity optimization is presented in [7]. In the general approach, the average dexterity of the robot is optimized over all its workspace. This method is more general as it does not depend on a specific configuration of the robot. Other works that optimize the dexterity of parallel robot are given in [8–13].

Another research direction related to structure optimization introduces the concept of kinematic isotropy of a robotic structure. This concept is investigated in [14–16] for the design process of planar and spherical parallel robots. In [17] the authors model a parallel manipulator with its legs as elastic members under axial loading. The authors propose the concept of the flexibility ellipsoid for a parallel system. The authors introduce various formulations of scalar measures of robots rigidity, which are based on the proposed ellipsoid. The authors also introduce an algorithm which decides upon some important design parameters of a generalized 6 DOF Stewart–Gough platform type parallel manipulator this algorithm involves multiple objective nonlinear programming techniques. In [18] the authors use the condition number of the Jacobian matrix of a 6×6 Stewart–Gough platform in order to optimize the kinematic design of a robot with respect to its isotropy. In [19] the authors identify the existence of two Jacobian matrices that result from kinematic analysis of a parallel robot. These matrices are related to the forward and inverse kinematics analysis. Hence the optimization process, which relies on formulating the condition number of the Jacobian matrix, involves the simultaneous minimization of two condition numbers relating to the two matrices.

In these previous works most of the methods presented are platform pose and/or configuration dependent, but they make no explicit use of available pre-knowledge relating to the ITD under consideration. This extra information, as will be shown here, can affect the final design and operation of the robot. Our suggested algorithm indicates the optimal platform pose and geometrical parameters of the parallel robot with respect to a given ITD. This algorithm can serve as another criterion, besides accuracy, rigidity, etc, to consider when optimizing a robot geometrical dimension or platform pose. We define an objective function that quantifies the total instantaneous work that is generated by the robot in a given ITD direction, while the task is represented in its screw parameters. The objective function includes the robot's geometrical and/or pose parameters as unknown, and is defined as the sum of the reciprocal product of the twist deformation, given in its screw representation, with the instantaneous wrenches that are applied to the platform by the robots' structure. These wrenches are the rows of the Jacobian matrix, that maps the external wrenches acting on the moving platform to the internal forces/moments (wrench) generated by the robot structure. The geometrical and/or location parameters are determined by solving for the extreme values of the objective function. This method is applicable during the design of a task-oriented new robot or while performing an ITD with a given robot. Moreover, this method can also be used with a reconfigurable robotic structure, capable of changing its geometry while performing the ITD. It should be mentioned that even though robots are generally defined as a general purpose tool, there are cases such as in the medical field where a robot is developed for a known group of predetermined tasks. In these cases, it is recommended to optimize the robot for the typical specifications of the assigned tasks [20].

2. Background

It has been shown [1] that the rows of the Jacobian of a parallel robot (columns for serial) are wrenches, which can be geometrically interpreted as Plücker line coordinates of lines. For example, when dealing with the classical 6×6 Gough–Stewart platform these lines are along the six limbs of the manipulator and describe the instantaneous forces of actuation applied by the robot structure on the upper moving platform. This is also the case when dealing with parallel robots having less than 6 DOF. In these cases, the set of static equilibrium equations for the moving platform results in a 6×6 Jacobian matrix whose rows are also wrenches, geometrically interpreted as Plücker line coordinates of lines that describe the actuation forces and moments of constraints which are applied to the platform [4,21,22]. These forces and torques are given in their screw coordinates and are also known as the governing line of mechanism. Next is a short overview of the tools that are used later in this report.

2.1. Plücker coordinates of a line, twist and wrench

A line is a geometric element that needs not more than four independent coordinates, therefore there being ∞^4 lines in space [23]. One way of describing a line is by using its Plücker coordinates [24]. A line can be defined by two given points, this definition is called 'homogeneous Plücker coordinates'. These coordinates are given by:

$$L = (x_0 y - y_0 x; x \times y) = (l, \bar{l}) = (p_{01}, p_{02,}, p_{03}, p_{23}, p_{31}, p_{12}) \tag{1}$$

where $X = (x_0, \ldots, x_3) = (x_0, x)$ and $Y = (y_0, \ldots, y_3) = (y_0, y)$ are two pints given in their homogeneous representation: $x, y \in \Re^3$ and $x_0, y_0 \in \Re$. These coordinates satisfy Klein's equation [24] and are contained in the Klein quadric M_2^4 [25]. Klein's equation is given by:

$$p_{01}p_{23} + p_{02}p_{31} + p_{03}p_{12} = 0 \tag{2}$$

It is worth noting that the lines $(p_{01}, p_{02,}, p_{03}, p_{23}, p_{31}, p_{12})$ and $\rho(p_{01}, p_{02,}, p_{03}, p_{23}, p_{31}, p_{12})$ are similar with ρ being a multiplier common to all the coordinates [23].

A rigid body displacement, i.e., a twist deformation, in E^3 can be represented by a screw motion about and along the same axis where the pitch, λ, of the motion is defined as the ratio of the translation, d, to the rotation, θ, for finite displacements, and the ratio of the instantaneous translation, $\dot{d}$, to the instantaneous rotation, $\dot{\theta}$, for an infinitesimal displacement. In order to represent a screw, $\hat{\$}$, it is convenient to use a screw coordinate system composed of two vectors [26,27], where s is a unit vector in the direction of the screw axis and s_0 is a position vector of a point on the screw axis. The Plücker coordinates of a line can be related to a twist as follows:

$$\hat{\$} = \begin{bmatrix} p_{01} \\ p_{02} \\ p_{03} \\ p_{23}^* \\ p_{31}^* \\ p_{12}^* \end{bmatrix} = \begin{bmatrix} S_1 \\ S_2 \\ S_3 \\ S_4 - \lambda S_1 \\ S_5 - \lambda S_2 \\ S_6 - \lambda S_3 \end{bmatrix} = \begin{bmatrix} s \\ s_0 \times s + \lambda s \end{bmatrix} = \begin{bmatrix} u \\ v^* \end{bmatrix} \tag{3}$$

The cross product $s_0 \times s$ is the moment of the screw axis relative to the origin of the reference frame. Since both the screw axis and the moment are directed at right angle to one another, their dot product is identically zero. Therefore they satisfy Eq. (2). Moreover, a pure rotation is represented as a zero pitch ($\lambda = 0$) screw (a line in Plücker coordinates) and a linear translation ($\lambda = \infty$) is represented as an infinite pitch screw which also corresponds to a line at infinity. The displacement of a rigid body cannot be completely determined without the specification of the amplitude or intensity of the screw axis. Let $\dot{q}$ be the intensity of a twist then the twist can be expressed as $\$ = \dot{q}\hat{\$}$ where $\dot{q} = \dot{\theta}$ for a pure rotation and $\dot{q} = \dot{d}$ for a pure translation.

The same description can be applied to representing a wrench. It has been shown that one can reduce a system of forces and couples acting on a rigid body, to a resultant force and couple about any point of interest.

In general the resultant force and couple are not collinear; however, it is possible to find a unique axis for both the resulting force, f, and the resulting couple, c. This force–couple combination is termed a wrench [27,28]. The unique axis is termed the wrench axis or screw axis of the system of forces and couples. The pitch of the wrench is defined as the ratio of the couple to the force.

The Plücker coordinates of a line can be related to a unit wrench as:

$$\hat{\$}_r = \begin{bmatrix} p_{01} \\ p_{02} \\ p_{03} \\ p^*_{23} \\ p^*_{31} \\ p^*_{12} \end{bmatrix} = \begin{bmatrix} S_{r1} \\ S_{r2} \\ S_{r3} \\ S_{r4} - \lambda_r S_{r1} \\ S_{r5} - \lambda_r S_{r2} \\ S_{r6} - \lambda_r S_{r3} \end{bmatrix} = \begin{bmatrix} s_r \\ s_{r0} \times s_r + \lambda_r s_r \end{bmatrix} \tag{4}$$

where s_r is a unit vector in the screw-axis direction and s_{r0} is a position vector of any point on the screw axis. The vector $s_{r0} \times s_r$ defines the moment of the screw axis with respect to the origin. For a pure force $\lambda_r = 0$ (a line) and for a pure couple $\lambda_r = \infty$ (a line at infinity). A wrench of intensity ρ is expressed by $\$_r = \rho\hat{\$}_r$.

2.2. Reciprocal screws

The concept of reciprocal screw was first introduced by Ball [26], and later in [29,23,27], and others. The main idea behind this concept is that if a wrench acts on a rigid body in such a way that it produces no work while the body undergoes an infinitesimal twist, then both screws representing the twist and the wrench are considered reciprocal to each other.

As can be seen in Fig. 1, a wrench $\$_r = \rho\hat{\$}_r$ is acting on a rigid body that undergoes a twist $\$ = \dot{q}\hat{\$}$. The virtual work between the twist and the wrench is given in [23] as:

$$\delta W = \rho\dot{q}[s \cdot (s_{r0} \times s_r + \lambda_r s_r) + s_r(s_0 \times s + \lambda s)] \tag{5}$$

where $s \cdot (s_{r0} \times s_r + \lambda_r s_r)$ is the multiplication of the instantaneous angular velocity and the instantaneous torque, respectively, and $s_r \cdot (s_0 \times s + \lambda s)$ is the multiplication of the instantaneous force with the instantaneous linear velocity, respectively; both multiplications result in instantaneous work. Observing the geometry of the system as is given in Fig. 1, Eq. (5) can be written as:

$$\delta W = \rho\dot{q}((\lambda + \lambda_r)\cos\alpha - a\sin\alpha) \tag{6}$$

In the case where $\delta W = 0$, then the wrench does not produce any instantaneous work while the body undergoes an instantaneous infinitesimal twist. Since Eq. (6) is symmetrical in λ and λ_r, the two screws can be interchanged without affecting their mutual reciprocal product. Moreover, in case of a pure rotation and pure force, i.e., $\lambda = \lambda_r = 0$, the two screws represent lines (see Eqs. (3) and (4)) and the reciprocal product results in $-a\sin\alpha$ where a is the distance between the two lines representing the screws axes and α is their mutual

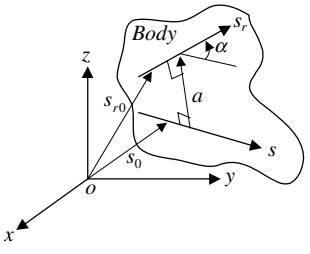

Fig. 1. Twist s and wrench s_r acting on a body [22].

angle. The same holds for pure moments and pure translations, where $\lambda = \lambda_r = \infty$ which corresponds to two lines at infinity that always intersect each other at infinity.

3. Synthesis algorithm

Without loss of generality we demonstrate our method using the classical Stewart–Gough platform; however the algorithm is general and can be applied to any structure.

Let us start by deriving the robot Jacobian matrix resulting from Static equilibrium conditions for the moving platform (see Fig. 2).

When writing the sum of forces and the sum of torques on the platform, one obtains:

$$\begin{aligned} &\sum_{i=1}^{6} f_i \hat{s}_i - F_{\mathrm{e}} = 0 \\ &\sum_{i=1}^{6} R\hat{r}_i \times f_i \hat{s}_i - M_{\mathrm{e}} = 0 \end{aligned} \tag{7}$$

where (see Fig. 2) $\hat{s}_i$ is a unit vector in the sliding direction of the prismatic joint of limb i. f_i is a scalar, representing the force along limb i. F_{e}, M_{e} are external forces and torques applied on the moving platform, and r_i is a radius vector from the origin of the platform coordinate frame, to the center of the spherical joint of limb i, written in platform coordinate frame as $r_p = [r_x, r_y, r_z, 1]^{\mathrm{T}}$ (T stands for transpose).

Also R is the rotational part of the homogeneous transformation matrix from platform coordinate frame to world coordinate frame (usually base platform coordinate frame) defined as

$${}^{w}R_p = \begin{bmatrix} R & p^{\mathrm{T}} \\ 0 & 1 \end{bmatrix} \tag{8}$$

where $p^{\mathrm{T}} = (p_x, p_y, p_z)^{\mathrm{T}}$ is a translation vector and R is a rotation matrix that can be obtained using screw representation, as a rotation of α radians relative to a 3D unit direction-vector denoted by $\vec{n} = (n_1, n_2, n_3)$. In this case, R is given as

$$R = \exp \alpha \cdot \begin{pmatrix} 0 & -n_3 & n_2 \\ n_3 & 0 & -n_1 \\ n_2 & n_1 & 0 \end{pmatrix} \tag{9}$$

where both p^{T} and $\vec{n}$ are defined in world coordinate system.

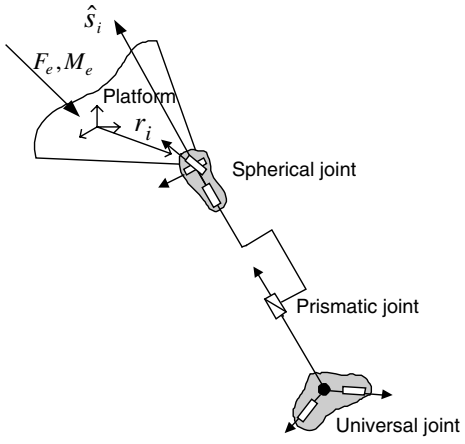

Fig. 2. Limb i of a Stewart–Gough platform.

Writing Eq. (7) in a matrix form yields:

$$\overbrace{\begin{bmatrix} \hat{s}_1 & \cdots & \hat{s}_6 \\ {}^{w}R_p\hat{r}_1 \times \hat{s}_1 & \cdots & {}^{w}R_p\hat{r}_6 \times \hat{s}_6 \end{bmatrix}}^{J^{\mathrm{T}}} \cdot \begin{bmatrix} f_1 \\ \vdots \\ f_6 \end{bmatrix} = \begin{bmatrix} F_{\mathrm{e}} \\ M_{\mathrm{e}} \end{bmatrix} \tag{10}$$

Given that

$$J^{\mathrm{T}} f = W_{\mathrm{e}} \tag{11}$$

where W_{e} is the external wrench (forces and torques) applied on the platform, then the parallel robot's Jacobian matrix, J^{T}, is given in Eq. (10). The first three components in each column correspond to the force and the last three to the torque generated to the moving platform by the corresponding limbs, hence one can also view the limbs of the Stewart–Gough platform as force generators [23]. For other type of parallel robots, the rows of the Jacobian are instantaneous wrenches applied on the platform. These wrenches can represent pure forces, pure torques or wrenches. This is true for any parallel robot, for ones with less than 6 DOF its Jacobian matrix is still ranked six, having three of the wrenches as moments of constraints and three as actuating forces [31]. It is worth noting that the Jacobian matrix of parallel robots is configuration dependent, i.e., it depends not only on the geometrical parameters of the robot, embedded in $\hat{s}_i$ and r_i, but also on the robot platform pose, i.e., location and orientation, as is reflected in ${}^{w}R_p$. We refer to the latter as pose parameters.

Next, we define an instantaneous twist deformation of the moving platform by its screw coordinates (ray coordinates) [24]; we term this the task. This definition is based on Eq. (3):

$$\chi[x, \bar{x}] = \begin{bmatrix} \hat{s} \\ s_0 \times \hat{s} + \lambda\hat{s} \end{bmatrix}^{\mathrm{T}} \tag{12}$$

where x represents the instantaneous angular deformation with units of $[1/t]$ (one divided by time) and $\bar{x}$ represents the instantaneous translation deformation with units of $[l/t]$, where l stands for unit of length and t for unit of time. We also write each of the rows of J in their ray coordinates as:

$$L_i = [j_i, \bar{j}_i] \tag{13}$$

where L_i represents row i of J, j_i represents the force i (first three numbers in row i) having units f (force) and $\bar{j}_i$ represents the torque i (last three numbers in row i) having units $f \cdot l$ (force · length).

Our objective function, F, is then defined as the sum of the square of the reciprocal product χ of Eq. (5) and L_i of Eq. (13) over i:

$$F = \sum_{i=1}^{6} (L_i \wedge \chi)^2 = \sum_{i=1}^{6} (\bar{j}_i \cdot x + j_i \cdot \bar{x})^2 = \overbrace{\sum_{i=1}^{6} (f \cdot l/s)^2 + (f \cdot l/s)^2 = (\mathrm{work}/s)^2}^{\mathrm{Units}} \tag{14}$$

Therefore, F is a scalar having units of the square of instantaneous work (power), and it describes the total instantaneous work generated by the robot structure on the moving platform while the latter undergoes an instantaneous twist motion defined by χ [4] in Eq. (12).

When defining F, one can set the geometrical parameters and/or the pose parameters as unknown a priori. We refer to these unknown parameters as the optimization unknown parameters.

Once both the optimization unknown parameters and the ITD, χ are determined, F can be derived and then, based on the design requirements, be maximized or minimized. The solution would be a set of optimal values for the optimization unknown parameters. When maximizing\minimizing the objective function, one obtains a set of optimization unknown parameters which maximize/minimize the instantaneous work generated by the robots' structure on its platform while the latter is undergoing the instantaneous motion characterized by the twist χ. In cases where the algorithm results in $F = 0$, the wrenches do not produce any work while the platform undergoes an infinitesimal twist, χ, meaning that the structure is in a singular configuration. This situation is characterized by a zero value for the objective function and a rank deficit Jacobian matrix of the robot [4].

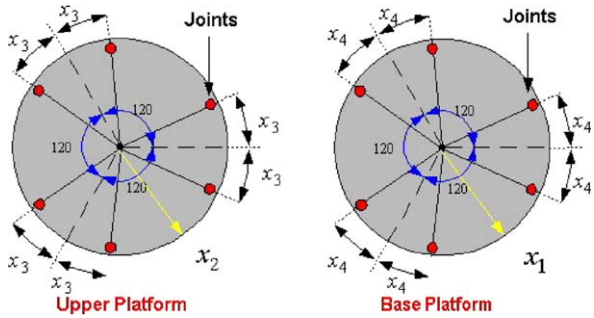

Fig. 3. Optimization parameters of a 6×6 Stewart–Gough platform.

Moreover, in case of a set of n predetermined ITDs, the optimization should be performed for each ITD separately, resulting in a set of n optimized optimization unknown parameters $q_i\,(x_j)_{i=1\ldots n}$ corresponding to each IDT $(x_j)_{j=1\ldots n}$. The final optimization unknown parameters are then calculated as the average of all sets (Eq. (15)) where w_i are weight factors (for each IDT), which correlate to the IDT frequency or its significance. These factors are to be determined by the designer based on his understanding of the process and ITDs under consideration.

$$Q = \sum_{i=1}^{n} \frac{w_i \cdot q_i(x_j)}{n} \tag{15}$$

In situations where one needs to design a robot for a specific predetermined ITD, this method can be used to determine the optimal combination of the robot geometrical parameters that would result in the extreme value for the objective function. In this case χ is known a priori and the optimization unknown parameters are those embedded in J, such as base and top platform dimensions, or joint distribution angles. Again, without loss of generality we present, in Fig. 3, examples of geometrical parameters for the Stewart–Gough platform for which x_1 and x_2 are the base and upper platform radius and x_3 and x_4 are the joint distribution angles on the base and upper platforms correspondingly.

The optimization method can also be used while operating a given robot. In this case, there can be two applications the first one is when given a robot with a fixed geometry and a given ITD, χ, to determine the platform pose parameters (e.g., position and orientation) that result in extreme values for F. In this case, the optimization unknown parameters are the elements of ${}^{w}R_p$, i.e., α, p^{T} and $\vec{n}$ of Eq. (10). The second application is when given a reconfigurable robot (i.e., capable of changing its geometrical parameters) and a task definition χ, determine both the robot geometrical parameters and its pose parameters that would result in extreme values of F. In this case, the unknown parameters are both α, p^{T}, $\vec{n}$ and $x_{1\ldots4}$ of the example illustrated in Fig. 3 for example.

Note that by optimizing the robot geometrical parameters for a specific task or set of tasks, the resulting robotic structure is likely demonstrate high performance capabilities while doing these tasks yet if for any reason the same robot is to be used for other different tasks, it is likely to perform relatively poorly. Hence, if one needs to design a robotic structure for a general undetermined task it is recommended to use other optimization methods that result in a more isotropic structure [14–16].

This method can be used as an extra criterion in the design phase and the operation phase of a robot.

4. Illustrative examples

In this section, we present several applications of the optimization algorithm. For the optimization process we use the Gauss–Newton optimization method. In each of the following examples the algorithm is provided with several starting points and the extreme solution was chosen, in order to try and avoid local minima [13]. Moreover, for each solution both the eigenvalues of the Hessian matrix and the partial derivatives of the objective function were calculated at the solution point to verify local optimum. Note that for clarity of presentation, the instantaneous screw axis corresponding to the ITD is plotted in a bold line in all the figures.

4.1. Optimizing a given structure for platform pose parameters

For this example, we are given the fixed geometry of the type of a Stewart–Gough platform: $x_1 = 12_{\text{cm}}$, $x_2 = 8_{\text{cm}}$, $x_3 = 30°$, $x_4 = 8°$ (Fig. 2). Moreover, the ITD, χ, is defined by

$$\hat{k} = [2, 2, 1]$$
$$k_0 = [2, 3, 6]_{\text{cm}}$$
$$\lambda = 1$$

i.e., it represents a combination of a translation and a rotation ($\lambda \neq 0, \infty$). The resulting ITD is $\chi = [2/3, 2/3, 1/3 - 1/3, 4, -1/3]$.

Next, we need to determine the robot platform pose parameters that result in extreme values of F, given χ.

Problem constraints (can be determined as needed):

$$-30° \leqslant \alpha \leqslant 30°, \quad -10_{\text{cm}} \leqslant p_{x,y} \leqslant 10_{\text{cm}}, \quad 20_{\text{cm}} \leqslant p_z \leqslant 50_{\text{cm}}$$

The resulting optimization parameters are (Fig. 4):

$$\left.\begin{aligned} &\vec{n} = [0, 0, 1] \\ &\alpha = -13.5° \\ &p = [-10, -10, 50]_{\text{cm}} \end{aligned}\right\} \text{Eq. (8), Eq. (9)}$$

In this case $F = 400.3$.

Next, we are given with the same parameters as in the previous example yet this time the ITD is represented by $\lambda = 0$, i.e., a pure rotation of the platform. This results in $\chi = [2/3, 2/3, 1/3 - 3, 10/3, -2/3]$.

Problem constraints are the same as before:

$$-30° \leqslant \alpha \leqslant 30°, \quad -10_{\text{cm}} \leqslant p_{x,y} \leqslant 10_{\text{cm}}, \quad 20_{\text{cm}} \leqslant p_z \leqslant 50_{\text{cm}}$$

The resulting parameters that maximize F are (Fig. 5):

$$\vec{n} = [0.3e^{-3}, 0.01, 0.74]$$
$$\alpha = -6.2°$$
$$p = [-10, -10, 50]_{\text{cm}}$$

In this case $F = 284.4$.

Note that a small change in task definition, i.e., pure rotation versus a combination of rotation and translation along the same screw axis, results in a different optimal platform pose. Also notice that the instantaneous work (F value) has dropped by about 30%, meaning worse performance of the platform for the ITD.

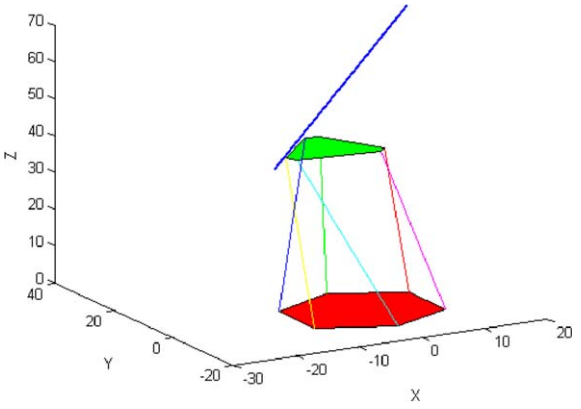

Fig. 4. Resulting robots' optimal platform pose, task direction is given in bold.

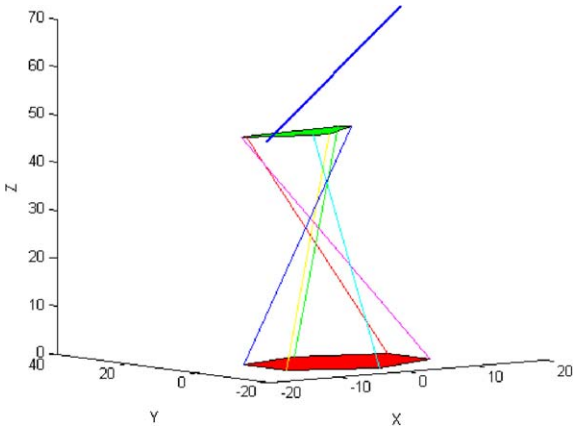

Fig. 5. Resulting robots' optimal platform pose, task direction is given in bold.

4.2. Optimizing a given structure for geometrical parameters

Our next example demonstrates the capability of the algorithm to identify also instantaneous singular configurations of a robot. In this example, we are looking for a Stewart–Gough platform geometry that is capable of generating maximum instantaneous power while simultaneously performing a pure instantaneous translation in a direction normal to the moving platform, and a minimum instantaneous power transmission while performing an instantaneous pure rotation with respect to the same normal (Fig. 6). This combination is sometimes required in assembly cells for "tie tolerance" peg-in-a-hole type of tasks. One of the common solutions to this problem is to provide the manipulator holding the peg with low angular rigidity and chamfer edges both to the peg and the hole [20].

The solution is obtained in two steps, i.e., by solving two sub-problems independently and then combining the two to a final solution (Eq. (15)). The first sub-problem is maximizing the instantaneous power while performing an ITD given by $\lambda = \infty$ in a normal direction to the platform. Eventhough the Jacobian is position dependent, we assume small motions of the platform hence while running the optimization, we keep the platform parallel to the base platform and in a fixed position $p = [0, 0, 40]_{\mathrm{cm}}$, resulting in $\chi = [0, 0, 1 - 10, -10, 0]$.

The second sub-problem is minimizing the instantaneous power transmission while performing a pure rotation (i.e., $\lambda = 0$) with respect to the same normal direction. Again we keep the platform parallel to the base platform and in the same fixed position $p = [0, 0, 40]_{\mathrm{cm}}$, resulting in $\chi = [0, 0, 0, 0, 0, 1]$.

Problem constraints; $2_{\mathrm{cm}} \leqslant x_1 \leqslant 6_{\mathrm{cm}}$, $2_{\mathrm{cm}} \leqslant x_2 \leqslant 6_{\mathrm{cm}}$, $0 \leqslant x_3 \leqslant 30°$, $0° \leqslant x_4 \leqslant 30°$.

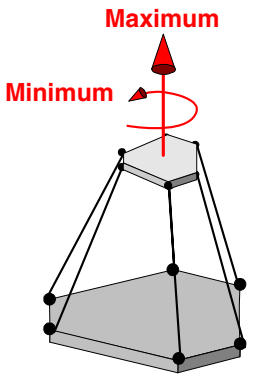

Fig. 6. Optimization requirements for maximum instantaneous work transmission in a perpendicular direction to the platform.

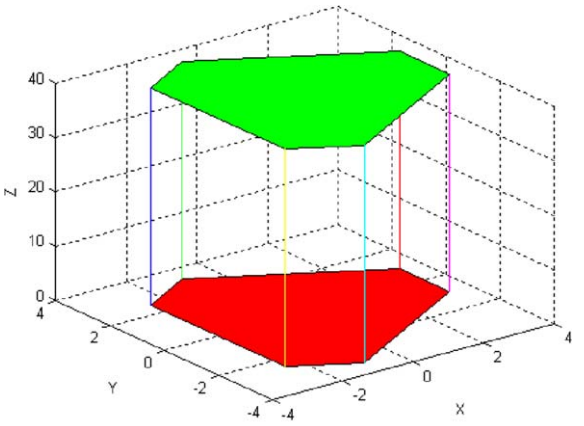

Fig. 7. Optimized geometry of the Stewart–Gough platform for peg-in-hole tasks.

The parameters obtained for both cases are (Fig. 6):

$$x_1 = 3.5_{\text{cm}}, \quad x_2 = 3.5_{\text{cm}}, \quad x_3 = 15^\circ, \quad x_4 = 15^\circ \text{ (rounded)}$$

with these parameters $F = 0$.

Note that in both cases the results indicate that the joints in both the base and moving platform are equally spaced. Moreover, both platforms are similar (Fig. 7), meaning that the structure is in architectural singularity. From line geometry point of view, all lines represented by the rows of the robots' Jacobian are parallel, and thus intersect at a common point at infinity forming a linear complex singularity of rank 3. Each line at infinity that intersects this point serves as the linear complex of the set of lines that describe the robot.

This example demonstrates that this method can be used to detect singular configurations of the robot by minimizing the objective function and looking for zero values of the latter. In these cases of a zero value for the objective function, there is no instantaneous work generated by the platform and the latter is in a singular configuration [4]. Normally, these configurations should be avoided unless they are utilized in the process such as in some remote compliance center mechanisms (RCC).

4.3. Optimizing for both pose and geometrical parameters

For this example, we are given a reconfigurable robot capable of changing the joint distribution angle on the upper platform, i.e., x_3 in Fig. 3, with the following geometric parameters: $x_1 = 12_{\text{cm}}, x_2 = 8_{\text{cm}}, x_4 = 30^\circ$.

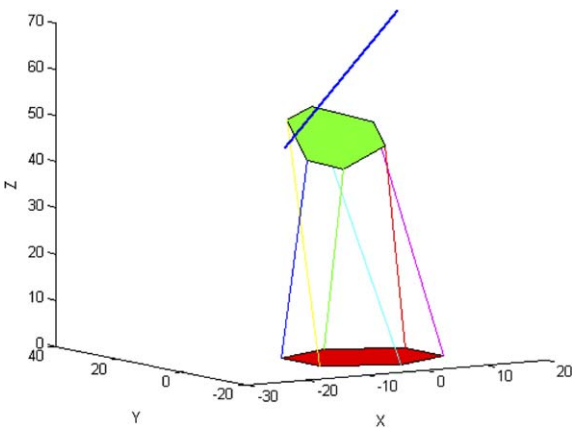

Fig. 8. Resulting robots' optimal platform pose, task direction is given in bold.

Moreover, we are also given the same ITD definition, χ as in Section 4.1 ($\lambda = 1$) resulting in $\chi = [2/3, 2/3, 1/3 - 1/3, 4, -1/3]$. We then solve for the robot geometrical and platform pose parameters, i.e., x_3, $\vec{n}$, α, p, which result in maximum values of F.

Constraints: $-30^\circ \leqslant \alpha \leqslant 30^\circ$, $-10_{\text{cm}} \leqslant p_{x,y} \leqslant 10_{\text{cm}}$, $20_{\text{cm}} \leqslant p_z \leqslant 50_{\text{cm}}$, $0^\circ \leqslant x_3 \leqslant 30^\circ$.

The resulting parameters are:

$$\vec{n} = [1, 0, 0]$$

$$\alpha = 4.3^\circ$$

$$p = [-10, -10, 50]_{\text{cm}}$$

$$x_3 = 21.1^\circ$$

In this case F gets a value of 524.7. Note that adding one extra geometric degree of freedom to the problem, i.e., x_3, results in a different distribution angle on the upper platform 8° versus 21.1°, and also a different pose of the platform (Fig. 8). More important, this extra degree of freedom results in a 23.7% increase in the instantaneous work generated by the moving platform in its ITD direction (400.3 versus 524.7).

4.4. The 3-UPU parallel robot geometrical parameters

The three DOF 3-UPU parallel mechanism first introduced in the literature by Tsai [32], have recently been the subject of kinematic analysis by several researchers [33,34,21]. Yet, it was only at the 2001 Computational Kinematics Workshop in Seoul that Park demonstrated on a working prototype which looked like a singular or a self motion behavior of the 3-UPU robot. In [21] the authors proved that at the home position of certain 3-UPU architectures, the corresponding lines of the manipulator are contained in two zero-pitch linear complexes (zero-pitch screw motions), resulting in a situation where an instantaneous two-parameter rotational motion about any line belongs to the line-pencil at the intersection point of the 3-UPU's limbs. Basically, this self motion is a result of a linear dependency of the robot's moments of constraints. These moments' directions are determined by the orientation of the upper universal joints that connect each of the three limbs to the moving platform. In this section, we reproduce the results obtained in [21] by choosing the IDF as one of the linear complexes singular direction in [21]. We expect the algorithm to result in a universal joint orientation that is collinear with the Park's singular manipulator in the case of minimal F values. Additionally, we use the same optimization definitions to find the orientation of these universal joints, for maximum F values.

In order to obtain the full 6×6 matrix that maps the external wrenches that are applied on the platform to the internal joints' reactions, the static equilibrium of forces and moments about the center of the moving platform is derived. These static equilibrium equations are given by (see Fig. 9 for definitions):

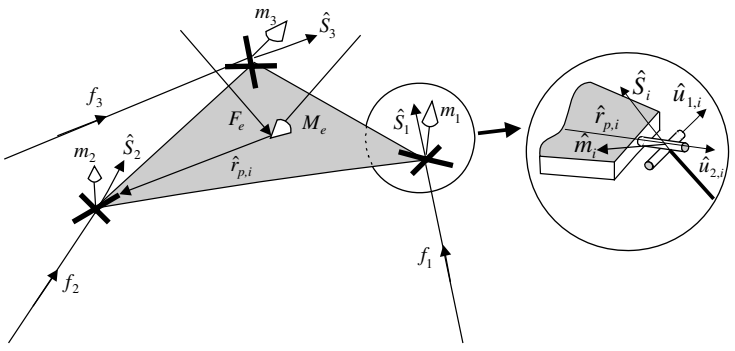

Fig. 9. Force and moment transmitted to the moving platform.

$$\sum_{i=1}^{3} f_i \hat{s}_i - F_e = 0$$
$$\sum_{i=1}^{3} m_i \hat{u}_i + \sum_{i=1}^{3} {}^{w}R_p \hat{r}_{p,i} \times f_i \cdot \hat{s}_i - M_e = 0 \tag{16}$$

where $\hat{u}_i$ is a unit vector normal to the two axes of the upper universal joint of limb i, $\hat{u}_{1,i}$ and $\hat{u}_{2,i}$ are unit vectors along the first and second axes of the upper universal joint of limb i, respectively, and ${}^{w}R_p$ is a rotation matrix from the platform coordinate system to world coordinate system located at the middle of the base platform.

Writing Eq. (16) in a matrix form yields:

$$\begin{bmatrix} \hat{s}_1 & \hat{s}_2 & \hat{s}_3 & 0 & 0 & 0 \\ {}^{w}R_p\hat{r}_{p,1} \times \hat{s}_1 & {}^{w}R_p\hat{r}_{p,2} \times \hat{s}_2 & {}^{w}R_p\hat{r}_{p,3} \times \hat{s}_3 & \hat{u}_1 & \hat{u}_2 & \hat{u}_3 \end{bmatrix} \begin{bmatrix} f_1 \\ f_2 \\ f_3 \\ m_1 \\ m_2 \\ m_3 \end{bmatrix} = \begin{bmatrix} F_e \\ M_e \end{bmatrix} \tag{17}$$

where

$$J^{T} = \begin{bmatrix} \hat{s}_1 & \hat{s}_2 & \hat{s}_3 & 0 & 0 & 0 \\ {}^{w}R_p\hat{r}_{p,1} \times \hat{s}_1 & {}^{w}R_p\hat{r}_{p,2} \times \hat{s}_2 & {}^{w}R_p\hat{r}_{p,3} \times \hat{s}_3 & \hat{u}_1 & \hat{u}_2 & \hat{u}_3 \end{bmatrix} \tag{18}$$

In [31] the authors identified that while in home position the lines of J belong to two axes of two zero-pitch linear complexes (linear congruence) given in their screw representation as (Fig. 10): $A_1 = [-0.94\ 0.35\ 0.0\ -34.6\ -93.9\ 0.0]$ and $A_2 = [0.35\ 0.94\ 0.0\ -93.9\ 34.6\ 0.0]$. The zero pitch indicates that the platform can perform an instantaneous pure rotation motion with A_1 and A_2 serving as axes of rotation. In order to demonstrate our concept, we run the optimization while keeping the geometrical parameters describing $\hat{u}_{1,i}$ and $\hat{u}_{2,i}$ $(i = 1 \ldots 3)$ as unknown (given in the platform coordinate frame), and the moving platform in home position. For the optimization we look for a set of geometrical parameters that minimize the objective function. The ITD definition χ is defined as A_1. The resulting $\hat{u}_{1,i}$ and $\hat{u}_{2,i}$ $(i = 1 \ldots 3)$ are:

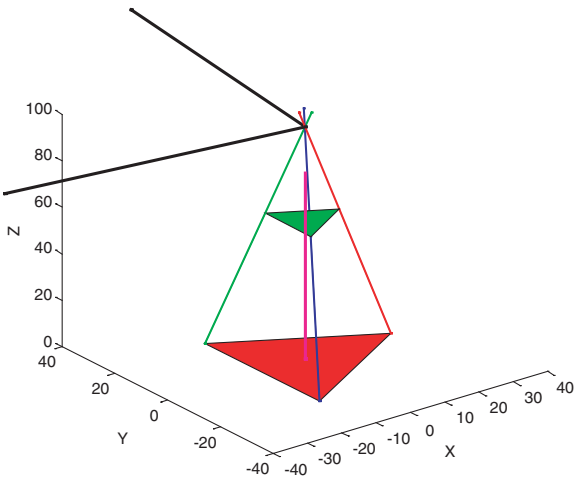

Fig. 10. 3-UPU–two zero-pitch screws axes in bold.

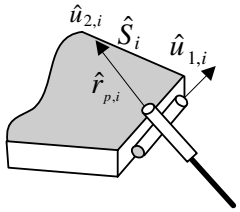

Fig. 11. Upper universal joint settings for maximum instantaneous power to upper platform in home position.

$$\hat{u}_{1,1} = [1, 0, 0]$$
$$\hat{u}_{2,1} = [0, -1, 0]$$
$$\hat{u}_{1,1} = [-0.5, 0.866, 0]$$
$$\hat{u}_{2,1} = [0.866, 0.5, 0]$$
$$\hat{u}_{1,1} = [-0.5, -0.866, 0]$$
$$\hat{u}_{2,1} = [-0.866, 0.5, 0]$$

and $F = 0$.

As expected the optimization results in the singular configuration of Park's robot $F = 0$. Next, we run the same simulation with the same task and same geometrical unknowns, yet this time we try to maximize the objective function.

The resulting $\hat{u}_{1,i}$ and $\hat{u}_{2,i}$ $(i = 1 \ldots 3)$ are:

$$\hat{u}_{1,1} = [0, -0.989, 0.012]$$
$$\hat{u}_{2,1} = [.91, 0, 0.03]$$
$$\hat{u}_{1,1} = [0.887, 0.51, 0]$$
$$\hat{u}_{2,1} = [-0.52, 0.856, 0]$$
$$\hat{u}_{1,1} = [-0.855, 0.49, 0]$$
$$\hat{u}_{2,1} = [-0.498, -0.846, 0]$$

and $F = 457.5$.

It is notable that the algorithm result, in a robot configuration in which the upper universal joint is rotated by 90°, meaning that the first and second revolute joints of the universal joints are switched which differs from Park's robot (Fig. 11). However, this robot configuration resembles the pure translational 3-UPU robot reported in [35]. Consequently, this robot is not capable of the rotations that were the instantaneous singular motions obtained by Park's design.

5. Conclusions

In this investigation we present an optimization method for optimizing the geometry and pose parameters of parallel robotic structures with respect to a predetermined ITD. The objective function is defined as the square of the sum of the reciprocal product of the instantaneous wrenches of the robot due to the ITD, which characterizes the task. The lines of the instantaneous wrenches are the rows of the Jacobian matrix of the robot, which describes the wrenches imposed on the robots' platform by its structure. Hence, the physical interpretation of the objective function is the square of the total instantaneous work generated by the robot's platform in the ITD direction. When maximizing/minimizing the objective function, one imposes a set of parameters which maximize/minimize the instantaneous work generated by the robot structure in the given ITD. When minimizing the objective function, the algorithm can also result in singular configurations of the structure, which corresponds to a zero value of the objective function. Normally, these configurations should be avoided.

This optimization method can be used in the design or operation stage of reconfigurable robots. In the paper, we present several examples in which we show how by adding degrees of freedom to the optimization (i.e., more parameters) can lead to an increase/decrease of the instantaneous work, i.e., better performances.

We suggest further analysis of the optimization algorithm be carried out by applying other local and global available optimization algorithms to the objective function described here. The comparison between algorithms should be on the basis of their efficiency, complexity, accuracy, and calculation time. However, when the robots' dimensions and locations are restricted due to mechanical concerns and ones' understanding of the task, then local optimization methods are sufficient as long as a post analysis and observation of the results is carried out. This method can be applied in the design stage of a robot or while performing the tasks, for example, by a reconfigurable robotic structure.

References

[1] J.P. Merlet, Singular configurations of parallel manipulators and Grassmann geometry, The International Journal of Robotics Research 8 (5) (1989) 45–56.
[2] B. Mayer St. Onge, C. Gosselin, Singularity analysis and representation of spatial six-dof parallel manipulators, in: Proceedings of Advances in Robot Kinematic, 1996, pp. 389–398.
[3] C. Gosselin, L. Perreault, C. Vaillancour, Simulation and computer-aided kinematic design of three-degree-of-freedom spherical parallel manipulators, Journal of Robotic Systems 12 (1995) 857–869.
[4] A. Wolf, M. Shoham, Investigation of parallel manipulators using linear complex approximation, ASME Journal of Mechanical Design 125 (September) (2003).
[5] C. Gosselin, M. Guillot, The synthesis of manipulators with prescribed workspace, ASME Journal of Mechanical Design 113 (4) (1991) 451–455.
[6] M. Tandirci, J. Angeles, F. Ranjbaran, The characteristic point and the characteristic length of robotic manipulators, in: Proceedings of the ASME Mechanisms Conference, DE-Vol. 45, 1992, pp. 203–208.
[7] C. Gosselin, J. Angeles, A global performance index for the kinematic optimization of robotic manipulators, ASME Journal of Mechanical Design 113 (3) (1991) 220–226.
[8] H. Pittens Kenneth, Ron P. Podhorodeski, A family of Stewart platforms with optimal dexterity, Journal of Robotic Systems 10 (4) (1993) 463–479.
[9] J.K. Salisbury, J.J. Craig, Articulated hand: force control and kinematic issues, The International Journal of Robotics Research 1 (1) (1982) 4–12.
[10] M. Togai, An application of the singular value decomposition to manipulability and sensitivity of industrial robots, SIAM 7 (2) (1986) 315–320.
[11] K.C. Gupta, B. Roth, Design considerations for manipulator Workspace, ASME Journal of Mechanical Design 104 (4) (1982) 704–712.
[12] R. Vijaykumar, M.J. Tsai, K.J. Waldron, Geometric optimization of manipulator structures for working volume and dexterity, The International Journal of Robotic Research 5 (2) (1986) 99–111.
[13] S.K. Advani, M.A. Nahon, N. Haeck, J. Albronda, Optimization of Six-Degrees-of-Freedom Motion Systems for Flight Simulators, American Institute of Aeronautics and Astronautics Inc., 1997.
[14] C. Gosselin, J. Angeles, The optimum design of a planar three-degree-of-freedom parallel manipulator, ASME Journal of Mechanisms Transmissions and Automation in Design 110 (1988) 35–41.
[15] C. Gosselin, E. Lavoie, On the kinematic design of spherical three-degree-of-freedom manipulators, International Journal of Robotics Research 12 (4) (1993) 394–402.
[16] H.R. Mohammadi Daniali, P.J. Zsombar-Murray, The design of isotropic planar parallel manipulators, in: Proceedings of the 1st World Automation Congress, Maui, vol. 2, 1994, pp. 273–280.
[17] S. Bhattacharya, H. Hatwal, A. Ghosh, On the optimum design of Stewart platform type parallel manipulators, Robotica 13 (1995) 133–140.
[18] K.E. Zanganeh, J. Angeles, Instantaneous kinematics of modular parallel manipulators, in: Proceedings of the ASME 23rd Mechanisms Conference, Minneapolis, DE-Vol. 72, 1995, pp. 271–277.
[19] C. Gosselin, J. Angeles, Singularity analysis of close loop kinematic chains, IEEE Journal of Robotics and Automation 6 (3) (1990) 281–290.
[20] Whitney, Navins, Concurrent Design of Products & Process, McGraw-Hill Publishing Company, 1989 (Chapter 7).
[21] A. Wolf, M. Shoham, F.C. Park, An investigation of the singularities and self-motions of the 3-UPU robot, in: Advances in Robots Kinematics, Kluwer Academic Publishers, 2002.
[22] M. Husty, A. Karger, H. Saches, W. Steinhilper, Kinematik und robotik, Springer, 1997.
[23] K.H. Hunt, Kinematic Geometry of Mechanisms, Department of Mechanical Engineering, Monash University, Clayton, Victoria, Australia, 1978.
[24] F. Klein, Ueber Liniengeometrie und metrische Geometrie, Mathematische Annalen v (1871) 257–303.
[25] H. Pottmann, M. Peternell, B. Ravani, An introduction to line geometry with applications, Computer Aided Design 31 (1999) 3–16.

[26] R.S. Ball, A Treatise on the Theory of Screws, Cambridge University Press, Cambridge, 1900.
[27] B. Roth, Screws, motors, and wrenches that cannot be bought in a hardware store, in: Proceedings of the 1st International Symposium of Robotics Research, 1984, pp. 679–693.
[28] M.S.C. Yuan, F. Freudenstein, L.S. Woo, Kinematic analysis of spatial mechanisms by means of screw coordinates, Part 1: Screw coordinates, ASME Journal of Engineering for Industry, Series B 93 (1) (1971) 61–66.
[29] K.J. Waldron, The Mobility of Linkage, Ph.D. dissertation, Department of Mechanical Engineering, Stanford University, Stanford CA, 1969.
[31] S.A. Joshi, L.W. Tsai, Jacobian analysis of limited-DOF parallel manipulators, Transaction of the ASME 124 (2002) 254–258.
[32] L.-W. Tsai, Kinematics of a three-DOF platform with three extensible limbs, in: J. Lenarcic, V. Parenti-Castelli (Eds.), Resent Advances in Robot Kinematics, 1996, pp. 401–410.
[33] R. Di Gregorio, V. Parenti-Castelli, A translational 3-DOF parallel manipulator, in: J. Lenarcic, M.L. Husty (Eds.), Advances in Robot Kinematics: Analysis and Control, Kluwer Academic Publishers, 1998, pp. 49–58.
[34] R. Di Gregorio, V. Parenti-Castelli, Mobility analysis of the 3-UPU parallel mechanism assembled for a pure translational motion, in: Proceedings of the IEEE/ASME International Conference on Advanced Intelligent Mechatronics, Atlanta, GA, September 19–23, 1999, pp. 520–525.
[35] R. Di-Gregorio, V. Parenti-Castelli, Mobility analysis of the 3UPU parallel mechanism assembled for a pure translation motion, Journal of Mechanical Design 124 (2002) 259–264.